

The harmonic oscillator at finite temperature using path integrals

Å. Larsen, and F. Ravndal

Citation: [American Journal of Physics](#) **56**, 1129 (1988); doi: 10.1119/1.15737

View online: <https://doi.org/10.1119/1.15737>

View Table of Contents: <https://aapt.scitation.org/toc/ajp/56/12>

Published by the [American Association of Physics Teachers](#)

ARTICLES YOU MAY BE INTERESTED IN

[Path integral for the quantum harmonic oscillator using elementary methods](#)

[American Journal of Physics](#) **66**, 537 (1998); <https://doi.org/10.1119/1.18896>

[Numerical Solution to Transient Heat Flow Problems](#)

[American Journal of Physics](#) **41**, 517 (1973); <https://doi.org/10.1119/1.1987281>

[Nonrelativistic contribution to Mercury's perihelion precession](#)

[American Journal of Physics](#) **47**, 531 (1979); <https://doi.org/10.1119/1.11779>

[On the harmonic oscillator inside an infinite potential well](#)

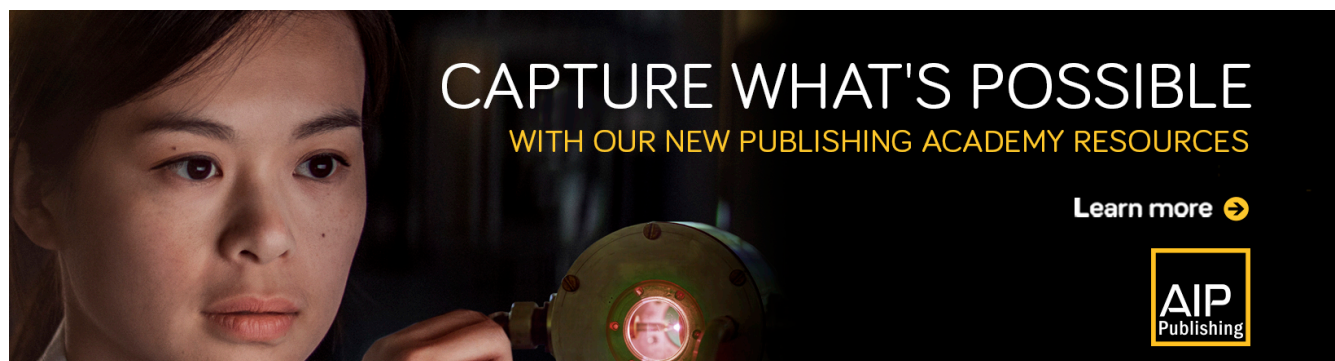
[American Journal of Physics](#) **56**, 1134 (1988); <https://doi.org/10.1119/1.15738>

[Critique and correction of the textbook comparison between classical and quantum harmonic oscillator probability densities](#)

[American Journal of Physics](#) **56**, 1123 (1988); <https://doi.org/10.1119/1.15736>

[The harmonic oscillator in quantum mechanics: A third way](#)

[American Journal of Physics](#) **77**, 253 (2009); <https://doi.org/10.1119/1.3042207>



cation. Our reconsideration of a standard introductory textbook theme shows that many generations of students have been exposed to a well-meant but unsuitable attempt of such an application to the important case of the harmonic oscillator, which has certainly hindered the process of understanding the workings of quantum mechanics much more than it has furthered it.

¹L. Pauling and E. B. Wilson, Jr., *Introduction to Quantum Mechanics* (McGraw-Hill, New York, 1935), p. 76.

²R. H. Dicke and J. P. Wittke, *Introduction to Quantum Mechanics* (Addison-Wesley, Reading, MA, 1960), p. 129.

³R. M. Eisberg, *Fundamentals of Modern Physics* (Wiley, New York, 1961), p. 264.

⁴L. I. Schiff, *Quantum Mechanics* (McGraw-Hill, New York, 1968), p. 74.

⁵A. Beiser, *Perspectives of Modern Physics* (McGraw-Hill, New York, 1969), Fig. 6.8.

⁶F. Bitter and H. A. Medicus, *Fields and Particles* (Elsevier, New York, 1973), pp. 238–239.

⁷R. Eisberg and R. Resnick, *Quantum Physics of Atoms, Molecules, Solids, Nuclei, and Particles* (Wiley, New York, 1974), p. 179.

⁸A. Böhm, *Quantum Mechanics* (Springer, New York, 1979), p. 60.

⁹R. Shankar, *Principles of Quantum Mechanics* (Plenum, New York, 1980), p. 212.

¹⁰P. Dennerly and A. Krzywicki, *Mathematics for Physicists* (Harper & Row, New York, 1967), p. 237.

The harmonic oscillator at finite temperature using path integrals

Å. Larsen and F. Ravndal

Institute of Physics, University of Oslo, Oslo 3, Norway

(Received 19 May 1987; accepted for publication 17 February 1988)

The statistical mechanics of a quantum harmonic oscillator can easily be formulated in terms of Feynman path integrals in imaginary time. By straightforward integrations, the partition function, the internal energy, and correlation functions are found. When time is discretized, the same results can be obtained directly using Monte Carlo methods on a computer. In the zero temperature limit, the usual quantum mechanical results are recovered.

I. INTRODUCTION

During the last decade, one has seen Feynman's formulation of quantum mechanics in terms of path integrals¹ arise from obscurity in the literature to the forefront of today's research in statistical physics and quantum field theory. In addition to being in many ways conceptually simpler than canonical methods involving noncommuting operators in some abstract Hilbert space, it is also ideally suited for numerical simulations on the powerful computers that are now generally available.

Among the many different Monte Carlo simulation methods, the Metropolis algorithm² seems in many ways to be the most popular, being fast and easy to translate into computer code. Its widespread use today is to a large extent due to its successful application in the ongoing investigations of quark confinement in lattice gauge theories.³

The same numerical methods can also be used in ordinary quantum mechanics⁴ and give a very concrete feeling of dynamical effects such as zero-point fluctuations and tunneling. Many of these effects can be investigated on an ordinary microcomputer and are suitable for undergraduate courses in quantum mechanics or computational physics.⁵

In order to implement a Feynman path integration on a computer, it is necessary to let the quantum mechanical system develop in imaginary time, preferably over a theoretically infinite time interval. Since this is in practice impossible on a finite computer, one actually ends up calculating finite temperature properties of the quantum

system.⁶ Nowadays, this is the standard method to obtain finite temperature results for interacting quantum field theories in numerical simulations.

Finite temperature quantum mechanics using path integrals is most easily explained using the harmonic oscillator as an example. The required formalism has already been developed by Creutz and Freedman,⁴ who used it primarily to derive zero temperature results. For their actual analytical calculations they went back to canonical methods using creation and annihilation operators for the oscillator. We think that it is more consistent and illustrative, especially for this simple system, to solve it completely using functional methods.

In Sec. II, we briefly outline how finite temperature properties of a quantum mechanical system can be found by functional integration over Feynman paths. This formalism is applied in Sec. III to the harmonic oscillator where all quantum fluctuations can be obtained directly. If the zero temperature limit is taken, one recovers the standard quantum mechanical results involving only the ground state. In Sec. IV some of these results are obtained from a Monte Carlo simulation based on the Metropolis algorithm and compared with the exact results we have at finite temperature on a finite lattice.

II. FINITE TEMPERATURE QUANTUM MECHANICS

For a quantum mechanical system with Hamiltonian

$$\hat{H} = (1/2m)\hat{p}^2 + V(\hat{q}) \quad (1)$$

in thermal equilibrium at temperature T , the partition function is

$$Z = \text{tr } e^{-\beta \hat{H}}, \quad (2)$$

with $\beta = 1/kT$. In the coordinate basis with $\langle q'|q \rangle = \delta(q' - q)$, the trace is simply the integral

$$Z(\beta) = \int_{-\infty}^{\infty} dq \langle q | e^{-\beta \hat{H}} | q \rangle. \quad (3)$$

Comparing the density matrix operator $\exp(-\beta \hat{H})$ with the time evolution operator $\exp(-it\hat{H}/\hbar)$, we see that the matrix element in (3) gives the transition amplitude for the particle to move from position q and back again to q in an imaginary time interval $it = \beta\hbar$.

In order to write (3) as a functional integral, we now repeat the standard procedure for real times.^{1,4,5} We partition the time interval $\beta\hbar$ into N segments, each of duration a so that $\beta\hbar = Na$. Inserting complete sets of coordinate eigenstates corresponding to each of these short time intervals, the original matrix element can be written as a product of N transition amplitudes of the form $\langle q' | \exp(-a\hat{H}/\hbar) | q \rangle$. In the limit where the lattice distance a is very small, one finds for the partition function

$$Z(\beta) = \int Dq \exp(-A[q]/\hbar). \quad (4)$$

Here,

$$\int Dq \equiv C^N \prod_{n=1}^N \int_{-\infty}^{\infty} dq_n \quad (5)$$

is the integration measure with $C = (m/2\pi a\hbar)^{1/2}$ and

$$A[q] = \sum_{n=1}^N a \left(\frac{m}{2a^2} (q_{n+1} - q_n)^2 + V(q_n) \right) \quad (6)$$

is the discretized expression of the action integral in imaginary time. Because of the trace in (2), we now have the periodic boundary condition $q_{N+1} = q_1$. A typical path or configuration in this approximation is shown in Fig. 1. In the limit $a \rightarrow 0$, $N \rightarrow \infty$ with β fixed, the action (6) takes the ordinary continuum form

$$A[q] = \int_0^{\beta\hbar} d\tau \left(\frac{m}{2} \dot{q}^2 + V(q) \right), \quad (7)$$

where τ is imaginary or Euclidean time equal to na when a is finite.

From the partition function $Z(\beta)$, we immediately obtain the free energy $F(\beta)$ from $Z = \exp(-\beta F)$. The internal energy $U(\beta)$ is the expectation value of the kinetic energy $T = -m\dot{q}^2/2$ plus the potential energy $V(q)$. From the virial theorem, one has

$$\langle T \rangle = \frac{1}{2} \langle qV' \rangle \quad (8)$$

for bounded motion. Expectation values are now calculated as in ordinary statistical mechanics. For example, the average potential energy is

$$\langle V \rangle = \frac{1}{Z} \int Dq V(q) e^{-A/\hbar}. \quad (9)$$

Instead of using the virial theorem, one can directly obtain the kinetic energy from the expectation value of the time-split product of the squared velocity,^{1,4}

$$\langle T \rangle = -m/2a^2 \langle (q_{n+1} - q_n)(q_n - q_{n-1}) \rangle, \quad (10)$$

where the different terms are given by the correlation function $C_{n-m} = \langle q_n q_m \rangle$.

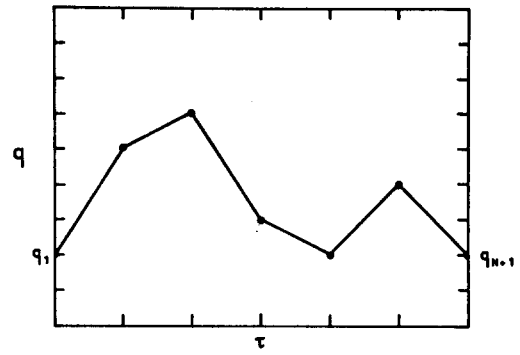


Fig. 1. The broken line is the discrete approximation to the path of a quantum particle going from q_1 to $q_{N+1} = q_1$.

In the zero temperature limit $\beta \rightarrow \infty$, the internal energy U equals the ground state energy E_0 . Taking this limit in the imaginary time formalism is in fact the method used to calculate ground state energies in numerical simulations.^{4,6}

III. THE HARMONIC OSCILLATOR

The path integral (4) for the partition function can be written as a product of simple Gaussian integrals for the harmonic oscillator with the potential $V(q) = \frac{1}{2}m\omega^2 q^2$. It can be evaluated directly⁷ using a recursive method. We will instead diagonalize the integrand by introducing the discrete Fourier components u_k of the position coordinates

$$q_n = N^{-1/2} \sum_{k=1}^N u_k e^{i(2\pi/N)kn}. \quad (11)$$

Using the completeness relation

$$\sum_{n=1}^N e^{i(2\pi/N)(k-k')n} = N \delta_{kk'}, \quad (12)$$

we also have the inverse transform

$$u_k = N^{-1/2} \sum_{n=1}^N q_n e^{-i(2\pi/N)kn}.$$

Requiring the coordinates q_n to be real restricts the number of independent, complex Fourier components u_k to equal N .

Now,

$$\sum_{n=1}^N q_n^2 = \sum_{k=1}^N u_k^* u_k$$

and

$$\sum_{n=1}^N (q_{n+1} - q_n)^2 = \sum_{k=1}^N 2u_k^* u_k \left(1 - \cos \frac{2\pi}{N} k \right)$$

so that the action (6) becomes diagonal:

$$A[q] = \frac{m}{2a} \sum_{k=1}^N u_k^* \left[2 \left(1 - \cos \frac{2\pi}{N} k \right) + a^2 \omega^2 \right] u_k. \quad (13)$$

The integration measure (5) is now

$$\int Dq = \Delta \int Du \equiv \Delta C^N \prod_{k=1}^N \int_{-\infty}^{\infty} du_k, \quad (14)$$

where the Jacobian $\Delta = |\partial q_n / \partial u_k|$. Using (11) and (12), one finds $\Delta \Delta^* = 1$, i.e., $\Delta = 1$.

The net result of the integration can be written as

$$Z(\beta) = (\det M)^{-1/2} \quad (15)$$

with

$$\det M = \prod_{k=1}^N \left[2 \left(1 - \cos \frac{2\pi}{N} k \right) + a^2 \omega^2 \right]. \quad (16)$$

Setting

$$\cosh x = 1 + \frac{1}{2} a^2 \omega^2$$

and

$$R = e^{-x} = 1 + \frac{1}{2} a^2 \omega^2 - a\omega(1 + \frac{1}{2} a^2 \omega^2)^{1/2}, \quad (17)$$

the product in the determinant (16) can be simplified using the identity

$$\prod_{k=1}^N \left(\cosh x - \cos \frac{2\pi}{N} k \right) = 2^{1-N} (\cosh Nx - 1), \quad (18)$$

which is derived in the Appendix. It gives

$$Z(\beta) = R^{N/2} / (1 - R^N). \quad (19)$$

We will also need the correlation function $C_s = \langle q_{n+s} q_n \rangle$. Using (11), we see that its Fourier transform is just the expectation value

$$\langle u_k^* u_k \rangle = \frac{a\hbar}{m} \frac{\delta_{kk'}}{2[1 - \cos(2\pi/N)k] + a^2 \omega^2},$$

which gives

$$C_s = \frac{a\hbar}{2Nm} \sum_{k=1}^N \frac{\cos(2\pi/N)ks}{\cosh x - \cos(2\pi/N)k}. \quad (20)$$

One way to carry out this summation is shown in the Appendix. We can write the result as

$$C_s = (\hbar/2m\Omega) [(R^s + R^{N-s}) / (1 - R^N)], \quad (21)$$

where

$$\Omega^2 = \omega^2 (1 + \frac{1}{2} a^2 \omega^2).$$

Our result for the correlation function together with (19) for the partition function was also derived by Creutz and Freedman⁴ using the transfer matrix and operator methods to diagonalize it.

Having found the correlation function for the oscillator quantum, we can now also calculate the internal energy U , which equals the sum $\langle T \rangle + \langle V \rangle$. For the potential energy, we have immediately

$$\langle V \rangle = \frac{1}{2} m \omega^2 C_0, \quad (22)$$

which will also be the result for $\langle T \rangle$ as seen from the virial theorem (8) when the potential is quadratic. Alternatively, we could have used the time-split expression (10) for the kinetic energy, which now gives

$$\langle T \rangle = (m/2a^2) (C_0 + C_2 - 2C_1). \quad (23)$$

Using the expression (21) for C_s , it is easy to see that this result is consistent with the virial theorem as long as $a\omega \ll 1$.

We can now check our expressions for the quantum harmonic oscillator at finite temperature against standard results derived from quantum mechanics in the continuous time limit where $a \rightarrow 0$, $N \rightarrow \infty$ with $Na = \beta\hbar$ finite. From (17), we then have $R^N = \exp(-\beta\hbar\omega)$. The partition function takes the well-known form

$$Z(\beta) = 1/2 \sinh(\frac{1}{2}\beta\hbar\omega),$$

i.e.,

$$Z(\beta) = \sum_{n=0}^{\infty} e^{-\beta\hbar\omega(n+1/2)}. \quad (24)$$

In this limit, we have recovered all the energy levels of the oscillator.

Similarly, the correlation function (21) simplifies to

$$C(\tau) = (\hbar/2m\omega) [\cosh(\frac{1}{2}\beta\hbar\omega - \omega\tau) / \sinh(\frac{1}{2}\beta\hbar\omega)], \quad (25)$$

where the time separation $\tau = sa$. The expectation value (22) of the potential energy is then

$$\langle V \rangle = \frac{1}{2} \hbar\omega \coth(\frac{1}{2}\beta\hbar\omega), \quad (26)$$

which will also be the expectation value of the kinetic energy. This consequence of the virial theorem follows again from (23) where we now on the right side simply have the double derivative of the correlation function, $\langle T \rangle = mC''(0)$. The total internal energy is therefore twice this result or

$$U = \frac{1}{2} \hbar\omega + \hbar\omega / (e^{\beta\hbar\omega} - 1). \quad (27)$$

In the zero temperature limit, $\beta \rightarrow \infty$, it is just the ground state energy $E_0 = \frac{1}{2} \hbar\omega$.

In numerical simulations, the ground state energy for a general potential can be obtained more directly from the partition function (3). Inserting a complete set of energy eigenstates, we see that

$$Z(\beta) \rightarrow \int dq |\psi_0(q)|^2 e^{-\beta E_0} \quad (28)$$

in the zero temperature limit $\beta \rightarrow \infty$. Here, $\psi_0(q)$ is the ground state wavefunction. Similarly, when the temperature is finite, the logarithm of the partition function gives directly the free energy. It was obtained along these lines in one of the earliest Monte Carlo simulations of the harmonic oscillator.⁶ In Sec. IV, we will present a few similar results based on the same algorithm.

IV. MONTE CARLO SIMULATION

In order to calculate expectation values like (9) numerically, we use the Metropolis algorithm. It is discussed in detail for this particular problem by Creutz and Freedman.⁴ Starting from some arbitrary configuration, as in Fig. 1, we choose to consider a point q_n . A random value q'_n is now generated in the interval $(q_n - \Delta, q_n + \Delta)$, where the width Δ is related to the time step a . It is introduced to avoid spending time on unimportant configurations. If the algorithm accepts this new value, q_n is replaced by q'_n . To improve convergence to equilibrium, this procedure was repeated a certain number of times \bar{n} on the same point q_n before proceeding to the next lattice point. In our simulation, we chose $\bar{n} = 5$. Going through all the points in the lattice is one Monte Carlo iteration. This new configuration can be updated again in further iterations.

After a certain number of iterations, thermal equilibrium is obtained. For our problem, it is easily characterized by having $\langle q_n \rangle = 0$, where the expectation value is now simply the average of q_n in a large set of such configurations. To avoid correlations between nearby configurations, we perform a few extra iterations between each of these measurements.

In our calculations, we decided to find the internal energy $U = \langle H \rangle$ of the oscillator. From the virial theorem (8), we know that it is simply the expectation value $U = m\omega^2 \langle q^2 \rangle$. From (21) and (22), we find

$$U = \frac{1}{2} \hbar\omega [\omega(1 + R^N) / \Omega(1 - R^N)]. \quad (29)$$

It is first calculated on lattices with $N = 4$ and 50 points, respectively, in the time direction. The results are shown in Fig. 2 together with the exact results. For $\beta\hbar\omega > 2$, we find very good agreement. This is obtained by first performing

500 iterations to obtain equilibrium and then averaging over 200–300 measurements with 5–10 intermediate iterations. With $N = 50$, we are in the continuum limit for these values of β ; increasing N does not noticeably change the results. In the zero temperature limit, $\beta \rightarrow \infty$, we recover the standard ground state energy $E_0 = \frac{1}{2}\hbar\omega$.

When $\beta\hbar\omega < 2$, i.e., at high temperatures, there are large fluctuations in the measured values and the agreement with the exact results is not too good. We discovered that in this region it took many more iterations to achieve thermal equilibrium; the results in Fig. 2 were obtained after 5000 iterations and with 20 intermediate iterations between each measurement. At these high temperatures, the system can be said to move much slower, the fast quantum fluctuations are now dominated by much slower thermal fluctuations.

In order to see how high temperatures slow the simulation, we show in Fig. 3 three typical equilibrium configurations with $N = 100$ at $\beta\hbar\omega = 50, 3$, and 0.6 . At very low temperatures, we see the fast quantum fluctuations around $q = 0$. At somewhat higher temperatures, $\beta\hbar\omega = 3$, the particle has a much slower thermal oscillation around $q = 0$ on top of which we see the much faster quantum fluctuations. With increasing temperatures, the thermal fluctuations become so slow that the whole configuration is in general displaced away from $q = 0$ as for $\beta\hbar\omega = 0.6$ in Fig. 3. Thermal averages in this region require a large ensemble of configurations separated by many iterations in

order to have thermal equilibrium with $\langle q \rangle = 0$. This takes relatively much time on a typical minicomputer.

These long relaxation times are a direct consequence of the physics of the system at high temperature. In the simulation, one then has a corresponding small lattice distance a in the time direction. Looking back at the action (6), one sees that this makes the kinetic energy more important relative to the potential energy. Since the change in the action must not be too large for an update of a coordinate to be accepted, it means that most resulting positions are very close to their original values. It takes correspondingly many more iterations to generate really different configurations. This is completely in accord with the picture one has about the high-temperature limit in statistical mechanics following from path integrals.¹

In order to check the calculations at high temperatures, we actually performed another Monte Carlo simulation on a larger and faster computer. We chose $N = 2$ since our analytical results then approximate very well the continuum limit when $\beta\hbar\omega < 1$. The necessary relaxation time to obtain thermal equilibrium increases rapidly with increasing temperatures. For $\beta\hbar\omega = 0.3$, we generated 100 000 configurations and measured for every 100 over the last 30 000 while for $\beta\hbar\omega = 0.2$ we used the last 120 000 con-

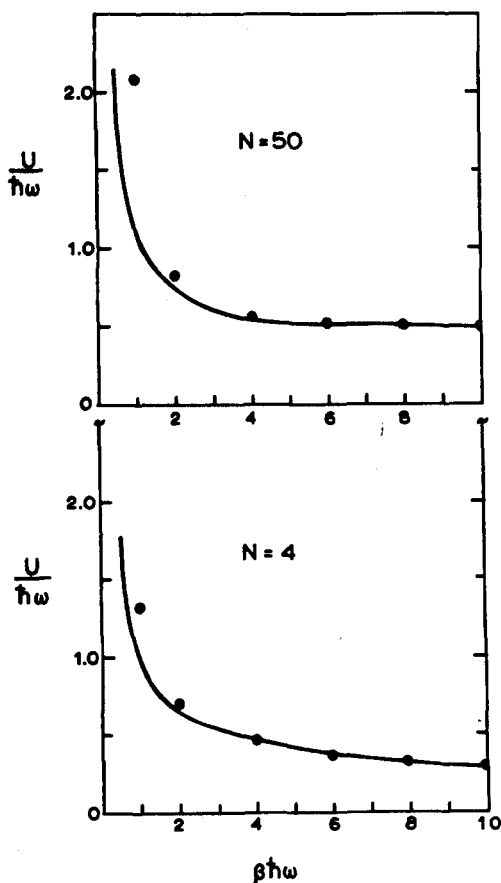


Fig. 2. Internal energies for the discretized harmonic oscillator at different temperatures. Points are from the Monte Carlo simulations while the curves represent the analytic expressions. The $N = 50$ results are almost indistinguishable from the continuum results at these temperatures.

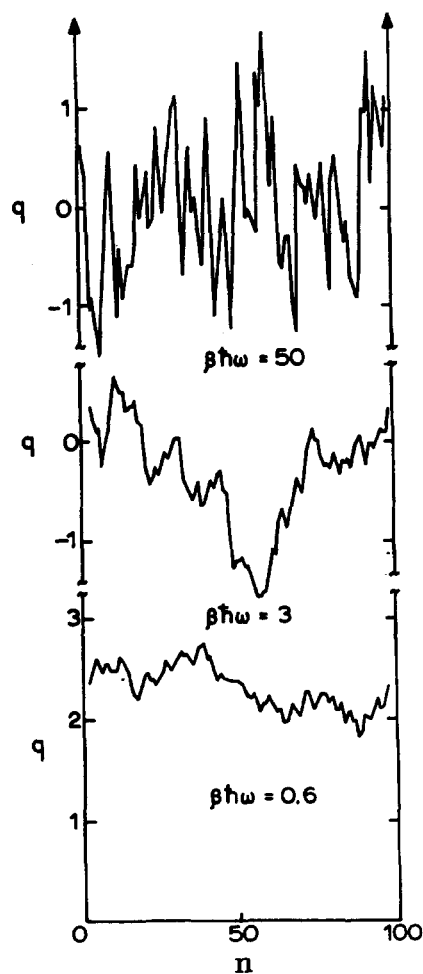


Fig. 3. Typical paths at three different temperatures obtained in the Monte Carlo simulation. While the points on the low-temperature path, $\beta\hbar\omega = 50$, are fluctuating around $q = 0$, they are all displaced away from the equilibrium position $q = 0$ at the high temperature $\beta\hbar\omega = 0.6$.

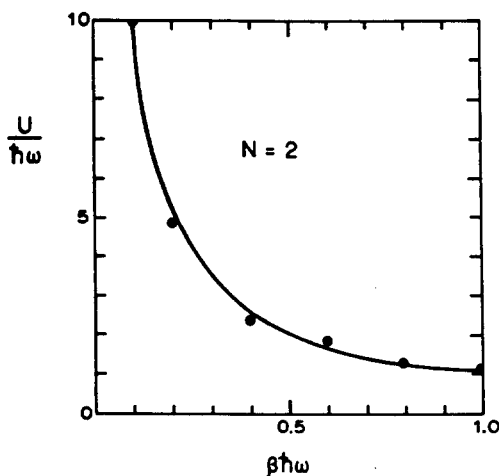


Fig. 4. High-temperature results for the internal energy. Points are from the Monte Carlo simulation. The curve represents the analytic expression. These $N = 2$ results are almost indistinguishable from the continuum results at these temperatures.

figurations in a series of 800 000 iterations. These high-temperature results are shown in Fig. 4. The numerical values all agree with the analytical ones to within 5%. We can conclude that the discrepancy in the high-temperature results presented in Fig. 2 is due to the relatively small number of configurations generated and used in calculating the averages.

V. DISCUSSION AND CONCLUSION

The harmonic oscillator at zero temperature has been for a long time an ideal example to illustrate the main properties of path integrals and to demonstrate the different mathematical methods required for their evaluation. This quantum mechanical problem is so simple and exactly solvable because the corresponding path integral is just an infinite product of ordinary Gaussian integrals. We have shown here that the same holds true at finite temperatures where one gets the results almost for free.

For this particular problem, the Monte Carlo simulations add little new at low temperatures. But it was somewhat surprising to find the very long amounts of time the system needed to reach equilibrium at higher temperatures. It gives a very good illustration of how the quantum and thermal fluctuations manifest themselves in a system of this type.

From these relatively long computer simulations required for this simple problem, one is led to question whether the Metropolis algorithm really is the optimal one for quantum mechanical systems where the number of degrees of freedom is so low. We chose to use this particular algorithm here since it ties in so naturally with the Feynman path integral. But today there are many other algorithms available that are used with great success in statistical mechanics and quantum field theory. It would be of interest to apply them to more elementary problems of the kind we have considered here.

APPENDIX

The identity (18) can be proven by considering the function $F(x) = \cos Nx - 1$. It has zeros for $x = (2\pi/N)k$,

$k = 1, 2, \dots, N$. Since $\cos Nx$ can be written as a polynomial of degree N in $\cos x$, we have immediately

$$\cos Nx - 1 = 2^{N-1} \prod_{k=1}^N \left(\cos x - \cos \frac{2\pi}{N} k \right), \quad (\text{A1})$$

where the prefactor is determined by comparing the coefficients of e^{Nx} on both sides. For $N = 2$, this identity represents a generalization of $\cos 2x - 1 = -2 \sin^2 x = 2(\cos x - 1)(\cos x + 1)$. Now letting x be imaginary, we have (18).

Using the Poisson summation formula, we can express the sum (20) as an infinite sum of the Fourier components F_n of the function

$$\begin{aligned} F(u, s) &= e^{isu} / (\cosh x - \cos u) \\ &= \sum_{n=-\infty}^{\infty} F_n(s) e^{inu}, \end{aligned} \quad (\text{A2})$$

i.e.,

$$F_n(s) = \int_0^{2\pi} \frac{du}{2\pi} F(u, s) e^{-inu}. \quad (\text{A3})$$

Now, choosing $u = (2\pi/N)k$ with $k = 1, 2, \dots, N$, we have

$$\sum_{k=1}^N F\left(\frac{2\pi}{N} k, s\right) = N \sum_{m=-\infty}^{\infty} F_{Nm}(s), \quad (\text{A4})$$

which is the desired summation formula. We have here used (12), which picks out the Fourier components $F_n(s)$ with $n = Nm$, $m = 0, \pm 1, \pm 2$ in the finite sum.

In our case, we see that $F_n(s) = f_{n-s}$, where f_n is the Fourier component of the simpler function $F(u, s=0)$, i.e.,

$$f_n = \int_0^{2\pi} \frac{du}{2\pi} \frac{e^{-inu}}{\cosh x - \cos u}. \quad (\text{A5})$$

This integral is most easily done introducing the variable $z = e^{iu}$, which translates it into a contour integral around $|z| = 1$ in the complex plane

$$f_n = 2 \oint \frac{dz}{2\pi i} \frac{z^{-n}}{(z - R)(R^{-1} - z)}. \quad (\text{A6})$$

Here, $R = e^{-x}$ as given in (17). Since $R < 1$, we have only one pole at $z = R$ when $n \leq 0$, giving $f_n = R^{-n}/a\Omega$. For $n > 0$, one similarly finds $f_n = R^n/a\Omega$. These two results can be combined to give, for all n ,

$$F_n(s) = R^{|n-s|}/a\Omega. \quad (\text{A7})$$

From (A4), we now see that the correlation function (10) is reduced to a geometric series

$$C_s = \frac{\hbar}{2m\Omega} \sum_{m=-\infty}^{\infty} R^{|Nm-s|},$$

which gives the result (21).

¹R. P. Feynman and A. R. Hibbs, *Quantum Mechanics and Path Integrals* (McGraw-Hill, New York, 1965).

²For some fascinating historical background, see H. L. Anderson, *J. Stat. Phys.* **43**, 731 (1986).

³M. Creutz, *Quarks, Gluons and Lattices* (Cambridge U. P., Cambridge, 1983).

⁴M. Creutz and B. Freedman, *Ann. Phys. (N.Y.)* **132**, 427 (1981).

⁵P. K. MacKeown, *Am. J. Phys.* **53**, 880 (1985).

⁶S. W. Lawande, C. A. Jensen, and H. L. Sahlin, *J. Comp. Phys.* **3**, 416 (1969).

⁷L. W. Bruch, *Chem. Phys. Lett.* **23**, 143 (1973).